

Comparison of Renormalization-Group and Lattice Studies of the Electroweak Phase Transition

N. Tetradis

*CERN, Theory Division,
CH-1211, Geneva 23, Switzerland*¹

Abstract

We compare the results of renormalization-group and lattice studies for the properties of the electroweak phase transition. This comparison reveals the mechanisms that underlie the phenomenology of the phase transition.

CERN-TH/96-331

November 1996

¹E-mail: tetradis@mail.cern.ch.

The most important consequence of the restoration of the electroweak symmetry at high temperatures [1] is related to the possibility that the baryon asymmetry of the Universe has been created during the electroweak phase transition [2]. The precise determination of the generated baryon number depends very sensitively on the details of the phase transition. This fact has instigated numerous studies of its characteristics during the last few years. (For recent reviews see ref. [3].) The perturbative approach for the determination of the temperature-dependent effective potential (from which the properties of the phase transition can be inferred) has been pursued up to two loops [4]. However, the perturbative expansion breaks down near and in the symmetric phase of gauge theories, due to the appearance of infrared divergences [5]. In order to overcome this difficulty, alternative approaches have been followed. Gap equations (truncated versions of Schwinger-Dyson equations) [6, 7] have been employed in order to obtain systematic resummations of infinite subclasses of perturbative contributions. The ϵ -expansion [8] has also been used in order to obtain insight into the non-perturbative character of the phase transition. The most reliable quantitative results have been obtained through the lattice approach [9]–[15]. However, the underlying dynamics that results in a certain physical behaviour is often obscured by the Monte-Carlo simulations. The analytical approaches offer a more intuitive understanding. Also, the requirement of long computer time for the simulations means that the exploration of the full phase diagram for a particular model is often a formidable task.

In ref. [16] a different approach has been followed, based on the exact renormalization group [17]. The method of the effective average action [18] has been employed. The effective average action Γ_k results from the integration of fluctuations with characteristic momenta larger than a given scale k (that can be identified with the coarse-graining scale of the system). This scale acts as an effective infrared regulator and gives control over the regions in momentum space from which divergences are expected to arise in perturbation theory. The dependence of Γ_k on k is described by an exact renormalization-group equation [19, 20]. For large values of k (of the order of the ultraviolet cutoff Λ of the theory) the effective average action is equal to the classical action (no fluctuations are integrated out), while for $k \rightarrow 0$ it becomes the standard effective action (all fluctuations are integrated out). As a result, the solution of the exact renormalization-group equation, with the classical action as initial condition, gives all the physically relevant information for the renormalized theory at low scales. The formalism is constructed in Euclidean space, which makes the consideration of temperature effects straightforward, through the imposition of periodic boundary conditions in the time direction (for bosonic fields) [21]. This approach has been used in the past for the discussion of the high-temperature phase transitions for the $O(N)$ -symmetric scalar theory [21, 22], multi-scalar theories [23], and the Abelian Higgs model [24, 25, 16]. The high-temperature phase transition for the $SU(2)$ Higgs model, which has all the qualitative characteristics of the electroweak phase transition, has been discussed in refs. [26, 27, 16]. The phase diagrams of the above models (with various fixed and tricritical points) have been determined in terms of the evolution of the potential, which incorporates all the running couplings of the theory. Non-

universal quantities (critical temperatures) as well as universal ones (critical exponents and amplitudes, the critical equation of state, crossover curves) have been computed. A description of the underlying mechanisms (such as dimensional reduction or radiative symmetry breaking) has been given. The use of the coarse-graining scale k has provided the necessary framework for the proper discussion of first-order phase transitions in the context of Langer's picture of nucleation [16, 28]. Overall, the method of the effective average action has provided a detailed and intuitive picture of the phase transitions in all the above field theories, without encountering any problem of infrared divergences. Effective theories of QCD have also been considered in ref. [29].

In this letter we compare the renormalization-group approach of ref. [16] with the lattice studies of refs. [9]–[14]. For this, we calculate the characteristics of the phase transition for the $SU(2)$ Higgs model, following the procedure presented in ref. [16], for the sets of parameters (gauge coupling, gauge and Higgs boson masses) used in refs. [9]–[14]. This comparison can be used in order to establish the level of accuracy of the renormalization-group approach. In spite of the clear and intuitive description of a large range of physical behaviours through the formalism of the effective average action, the quantitative accuracy of the results is not easily determined. This is due to the approximations that one has to employ in order to bring the exact renormalization-group equation for Γ_k into a manageable form that permits its solution. The largest source of uncertainty is introduced by the assumption for the invariants appearing in Γ_k . The most commonly employed ansatz is a truncated expression that keeps the full field and scale dependence of the potential, and two-derivative kinetic terms for the fields, but neglects higher derivative terms in the effective average action. An intrinsic estimate of the induced error requires a comparison with more extended truncations. An alternative way of checking the accuracy of the results is to compare them with the results of other approaches. For example, the accuracy of the critical exponents for the second-order phase transitions of the $O(N)$ -symmetric scalar theory, calculated in refs. [21, 22], has been determined through the comparison with ϵ -expansion results. This has permitted an estimate of the accuracy of the result for the critical equation of state. For the work of ref. [16], the comparison with the lattice calculations will lead to the understanding of the mechanisms underlying the phenomenology of the phase transition. These mechanisms are obscured by the Monte Carlo simulations, while they are clearly observed in the renormalization-group approach.

We give first a brief summary of the approach followed in ref. [16] for the study of the $SU(2)$ Higgs model with one doublet. An ansatz is employed for the effective average action, which includes a general effective average potential $U_k(\rho)$ for the scalar field ($\rho = \phi^\dagger\phi$), two-derivative kinetic terms and a gauge-fixing term. The anomalous dimension of the scalar field is neglected, while the wave-function renormalization of the gauge field is incorporated in the running gauge coupling $e^2(k, \rho)$. With the above approximations, the exact renormalization-group equation for the k dependence of Γ_k can be translated into evolution equations for $U_k(\rho)$ and $e^2(k, \rho)$. The temperature effects are taken into account through periodic boundary conditions in the imaginary-time direction. This leads

to the generalization of the evolution equations for the temperature-dependent $U_k(\rho, T)$ and $e^2(k, \rho, T)$. For $k \gg T$ the temperature effects are negligible and the evolution is typical of a four-dimensional, zero-temperature theory. For $k \ll T$ the evolution equations can be cast in a form typical of a three-dimensional, zero-temperature theory. This can be achieved if one defines effective three-dimensional parameters by multiplying with appropriate powers of T

$${}^3U_k(\rho_3) = \frac{U_k(\rho, T)}{T}, \quad \rho_3 = \frac{\rho}{T}, \quad e_3^2(k, \rho) = e^2(k, \rho, T)T, \quad (1)$$

and their dimensionless versions (rescaled by powers of k)

$$u_k(\tilde{\rho}) = \frac{{}^3U_k(\rho_3)}{k^3} = \frac{U_k(\rho, T)}{k^3 T}, \quad \tilde{\rho} = \frac{\rho_3}{k} = \frac{\rho}{kT}, \quad \tilde{e}^2(k, \rho) = \frac{e_3^2(k, \rho)}{k} = \frac{e^2(k, \rho, T)T}{k}. \quad (2)$$

The evolution equations are [20, 24, 16]

$$\frac{\partial u_k}{\partial t} = -3u_k + \tilde{\rho}u'_k - v_3 L_0^3(u'_k + 2u''_k \tilde{\rho}) - 3v_3 L_0^3(u'_k) - 6v_3 L_0^3(2\tilde{e}^2 \tilde{\rho}), \quad (3)$$

$$\frac{\partial \tilde{e}^2}{\partial t} = -\tilde{e}^2 - \frac{4}{3}v_3 88 \tilde{e}^4 l_{NA}^3 \theta(2\tilde{e}^2 \tilde{\rho}). \quad (4)$$

Here $t = \ln(k/\Lambda)$, $v_3 = 1/8\pi^2$, $l_{NA}^3 = 0.677$ and primes denote derivatives with respect to $\tilde{\rho}$. The ‘‘threshold’’ functions $L_0^3(w)$ take negative values, and fall off for large rescaled masses of the radial scalar, Goldstone and gauge modes that serve as their arguments. In the evolution equation for the gauge coupling the ‘‘threshold’’ function has been approximated by a θ -function. The various subscripts and superscripts set equal to 3 in the above expression indicate that the evolution is typical of a three-dimensional theory. We started with the evolution equation for the four-dimensional theory at non-zero temperature, and, for $k \ll T$, obtained the evolution equation for an effective three-dimensional theory at zero temperature. Thus we have obtained a realization of the mechanism of dimensional reduction. In ref. [16] the above equations were shown to be a very good approximation in the whole region $k \leq T$, for the parameter range of interest for the electroweak phase transition. The renormalized theory (for $k = 0$) at non-zero temperature is determined through their numerical integration with algorithms discussed in ref. [30]. The initial conditions at $k = T$ can be expressed in terms of the renormalized parameters of the zero-temperature theory at $k = 0$ (minimum of the potential ρ_{0R} , quartic coupling λ_R , and gauge coupling e_R^2 , or, equivalently, gauge and Higgs boson masses, and gauge coupling) and the temperature.

In fig. 1 we present the evolution of the effective average potential $U_k(\rho, T)$ for the $SU(2)$ Higgs model with $e_R^2 = 0.1073$, $m_W = 80.6$ GeV, $m_H = 35$ GeV, as the coarse-graining scale k is lowered. The temperature is chosen near the critical one. Initially the potential has only one minimum away from the origin, which receives a renormalization proportional to the running scale k during the evolution. At some point a new, shallow minimum appears at the origin. It is induced by the integration of thermal fluctuations,

through the generalization of the Coleman-Weinberg mechanism [31]. The evolution slows down at later stages and the potential converges towards a non-convex profile. With an appropriate choice of the coarse-graining scale k , this potential can be employed for the proper discussion of the properties of the first-order phase transition [16, 28]. During the same “time” t , the running gauge coupling $e^2(k, \rho, T)$ increases, because the $SU(2)$ Higgs model is asymptotically free. This evolution is stopped, however, because of the decoupling of the massive gauge field fluctuations when the running scale k becomes smaller than their mass $\sqrt{2e^2\rho}$. This decoupling takes place earlier for larger ρ , while for small values of ρ near the origin the gauge coupling continues to increase. Eventually it reaches a critical value, for which a confining regime is expected to emerge. An estimate for this value is $\alpha = 4\tilde{e}^2/4\pi = 1$. (The reason for the factor of 4 is our unconventional normalization of the gauge coupling.) We have stopped the evolution at this scale, which is determined through the expression ²

$$\tilde{e}^2(k_{conf}, \tilde{\rho} = 0) = \frac{e^2(k_{conf}, \rho = 0, T) T}{k_{conf}} = \pi. \quad (5)$$

The evolution for $k < k_{conf}$ cannot be reliably described in terms of a parametrization of the effective average action through fundamental fields. Instead, one has to use a basis of composite operators, corresponding to the bound states that are expected to form at these scales. The two formulations must be matched at $k = k_{conf}$ [32]. The various bound states are expected to be massive, with masses of the order of k_{conf} , and they should soon decouple. The most significant contribution from this last part of the evolution comes from the appearance of condensates associated with operators such as F^2 . In ref. [33] it was shown that F^2 develops a non-zero expectation value in the confining regime, with a reduction of the energy density compared to the state with $F^2 = 0$. This negative contribution affects the potential of fig. 1. The reason is that the strongly coupled regime appears only near the origin of the potential, where the running of the gauge coupling has not been cut off. We expect, therefore, a negative contribution to the potential for the region around $\rho = 0$ where the coupling satisfies eq. (5). On dimensional grounds, we can approximate the negative contribution to the potential by

$$\Delta U = - (ck_{conf})^3 T. \quad (6)$$

The phenomenological constant c is expected to be of order 1. We consider the values $c = 1$ and 0.5 in order to study the effect of this parameter on the characteristics of the phase transition. In fig. 1 we display the final form of the potential, if the above contribution with $c = 1$ is added to the result of the integration at $k = k_{conf}$. This term is added to the potential only in the small region around the origin where the running gauge coupling reaches the value determined by eq. (5). As a result, the shallow minimum at the origin becomes as deep as the minimum at non-zero ρ . We have not attempted to account for the ρ dependence of the F^2 condensate beyond a crude step-like behaviour,

² The value of k_{conf} is not very sensitive on its precise definition. The gauge coupling $\tilde{e}^2(k)$ becomes of order 1 at scales k within 10 % from the scale k_{div} at which it diverges.

by introducing additional phenomenological parameters. As our analysis cannot provide any hint on the value of these parameters, we have preferred to neglect them completely. This explains the steep rise of the potential of fig. 1 near the origin. Notice however that the influence of this crude approximation on the characteristics of the phase transition is rather small. For example, the latent heat is determined by the temperature dependence of the energy density at the minimum away from the origin. This depends on the value of the contribution of eq. (6), but not on its precise ρ dependence. Similarly, the surface tension involves an integration over the whole range between the two minima, which reduces the effect of our approximation.

In fig. 2 we present the evolution of the potential for $m_H = 70$ GeV and a temperature near the critical one. We observe the running of the minimum and the curvature at the origin becoming less negative. In the region around the origin, the running gauge coupling reaches the critical value of eq. (5), at which the confining regime is expected to set in. The size of this region relative to the location of the minimum of the potential is larger than in the case of fig. 1. Confinement sets in while the curvature at the origin is still negative and the Coleman-Weinberg mechanism has not yet become effective. At this point we stop the evolution and add the contribution of eq. (6) to the potential (here we have used $c = 0.5$), in the region around the origin where the coupling has the critical value. This results in a new minimum between the origin and the original minimum of the potential. A first-order phase transition is predicted, but both minima now exist at non-zero values of the Higgs field. Within the effective average action approach, the appearance of a minimum at a non-zero Higgs field expectation value has been observed for the first time in ref. [27], where a simplified version of the evolution equation for the potential has been used. Within the gap-equation approach, it has been observed in ref. [7]. For even larger scalar masses a qualitative change is expected. The evolution resembles that in fig. 2, until the gauge coupling reaches its critical value. When the strongly coupled regime sets in, its extent is larger than the location of the minimum of the potential. This indicates that no minimum exists any longer where the description in terms of fundamental fields is possible. The two-minimum structure of the potential is not expected to appear any more. Instead, the transition to a non-perturbative vacuum is expected to be continuous, without appearance of singularities. As a result no phase transition exists any more. This indicates the change from first-order phase transitions to analytical crossovers for large scalar masses. Our analysis predicts a critical scalar mass in the range 80–100 GeV. The possibility of a crossover for gauge theories has been first suggested in ref. [34]. For the electroweak phase transition, it has been observed in ref. [7], where the gap-equation approach has been followed. Within the effective average action approach, it has been observed in refs. [26, 27], where arguments similar to ours have been given for the first time. The most reliable and detailed results that confirm this possibility have been obtained through the lattice approach [35].

The characteristics of the phase transition can be deduced from the form of the potential, as explained in ref. [16]. In table 1 we present them for models with $m_W = 80.6$ GeV, and e_R^2 , m_H equal to the set of values employed in the lattice studies of refs. [9]–[14]. The

value $c = 1$ has been used in the contribution of eq. (6). We give the critical temperature, the location of the minimum away from the origin, the location of the confining minimum (whenever it appears), the scale k_{conf} where confinement sets in, the masses of the fields at the minimum away from the origin, the surface tension and the latent heat of the phase transition. All the above quantities have been extracted from the potential at $k = k_{conf}$ after the addition of the contribution of eq. (6). The surface tension has been calculated through the leading semiclassical thermal-tunnelling fluctuation [16]. We do not give any values for the masses of the fields at the origin. There, the proper description should include bound states instead of fundamental fields; this is the subject of future work.

In table 2 we compare the renormalization-group results with those of lattice and perturbative studies for $e_R^2 = 0.1463$, $m_W = 80.6$ GeV, $m_H = 34$ GeV. We consider the critical temperature, surface tension and latent heat that are discussed in refs. [10, 11, 14]. The discontinuity in the Higgs field expectation value in table 1 corresponds to expectation values of ϕ in a formalism with gauge fixing. This is not comparable to the discontinuity of the expectation value of the operator $\phi^\dagger\phi$ that is calculated in the lattice studies. The first column (RG1) results from the integration of the evolution equation for the potential, with the contribution of the strongly coupled regime around the origin approximated by eq. (6) with $c = 1$. For the second column (RG2) we have used $c = 0.5$. The comparison of the two columns gives an estimate of the effect of the confining regime on the properties of the phase transition. It is apparent from figs. 1 and 2 that the addition of the contribution of eq. (6) results in a more strongly first-order phase transition. This effect is enhanced for larger c , and is reflected in the larger values of σ/T_{cr}^3 and $\Delta Q/T_{cr}^4$. In the third column (L1) we give the results of the lattice study of refs. [10, 11]. The continuum limit $L_t = \infty$ has been studied only for T_{cr} . For the surface tension and latent heat we list the finite-lattice results. In the fourth column (L2) we list values that have been obtained in ref. [14] through the extrapolation of the results of ref. [13] to the value $m_H = 34$ GeV. These results have been obtained through numerical simulations of the effective three-dimensional theory, so that the continuum limit for the time direction is not needed. Finally in the last two columns we give the perturbative predictions to order g^3 (PT1) and g^4 (PT2) [11]. We observe that the RG1, RG2 predictions for the critical temperature are larger than the L1, L2 results, but smaller than the PT1, PT2 predictions. Moreover, the RG1 prediction is significantly closer to the lattice results. This indicates that the value $c = 1$ is the preferred one. This choice is further supported by the comparison of the results for the surface tension and latent heat. For $c = 1$, the non-perturbative effects dramatically increase the strength of the phase transition. Their influence is much larger than that due to the growth of the running gauge coupling. This effect has been estimated in ref. [16], where the form of the potential at the critical temperature has been calculated, without and with the running of the gauge coupling (by considering a zero β -function for the gauge coupling, or by employing eq. (4)). As the first-order phase transition is triggered by the gauge-field fluctuations, its strength is increased when the running of the gauge coupling is taken into account. An increase in the strength of the phase transition is observed in higher orders of perturbation theory (compare columns

PT1 and PT2). However, the agreement of column PT2 with the lattice results cannot be explained by our analysis. Our fig. 1 indicates that the non-perturbative effects of the strongly-coupled regime are substantial already at $m_H = 35$ GeV. In summary, we conclude that, for scalar masses around 35 GeV, the characteristics of the first-order phase transition are properly reproduced by our analysis, if the non-perturbative contribution from the strongly-coupled regime in the evolution of the potential is approximated by eq. (6) with $c = 1$. We should point out, however, that the determination of the value $c = 1$ through an explicit calculation in the context of the effective average action is pending.

In table 3 we compare the renormalization-group approach with the lattice studies for several scalar masses. We observe that the choice $c = 1$ in eq. (6) leads to a good description of the phase transition for light Higgs bosons with $m_H = 29.1, 34$ GeV. For larger m_H the agreement between renormalization-group and lattice results becomes much weaker. The discrepancy is most obvious for the surface tension. This quantity is the most difficult to extract from the renormalization-group calculation for large m_H , when the phase transition becomes very weakly first order. This is apparent in fig. 2, where there is no interval in the evolution during which the potential converges towards a stable non-convex profile (in contrast to fig. 1). The determination of the surface tension from the potential, through a semiclassical tunnelling solution, is very sensitive to the choice of coarse-graining scale. This indicates that the contribution to the tunnelling rate coming from fluctuations around the semiclassical solution is important and must be taken into account [28]. Also the step-like behaviour of the potential of fig. 2 becomes a very crude approximation. As a result, the values for the surface tension, obtained through the renormalization-group approach for $m_H = 49, 54.4$ GeV, are subject to large uncertainties. It should also be pointed out that the sensitivity of the surface tension and latent heat on the choice of c in eq. (6) is large for $m_H = 49, 54.4$ GeV. A value $c = 0.5$ leads to the necessary reduction of σ/T_{cr}^3 and $\Delta Q/T_{cr}^4$. However, it also leads to a much larger value of T_{cr} than the choice $c = 1$.

In fig. 3 we plot the location of the two minima of the potential at the critical temperature, as a function of the scalar mass, for $m_W = 80.6$ GeV. The data of table 1 have been used, as well as those of ref. [16]. An additional calculation has provided the points at $m_H = 40$ GeV. The stars correspond to $e_R^2 \simeq 0.145$ and the boxes to $e_R^2 \simeq 0.107$. The white boxes for $m_H = 70$ GeV are only indicative, as the quantitative reliability of the results is small for $m_H \gtrsim 55$ GeV. An extrapolation of the two lines of data for the two minima of the potential indicates that they should coincide for a Higgs mass in the range 80–100 GeV. This is the range in which an analytical crossover is expected to set in. However, a detailed description of the system in this range requires the parametrization of the effective average action in terms of composite operators, corresponding to the bound states that are expected to appear.

In conclusion, the comparison of renormalization-group and lattice studies reveals the mechanisms underlying the phenomenology of the electroweak phase transition. The Coleman-Weinberg mechanism operates for scalar masses $m_H \lesssim 40$ GeV. It generates a two-minimum structure in the potential and induces the first-order phase transition.

The strength of the phase transition is enhanced by the confining dynamics near the symmetric phase of the model, which increases the depth of the minimum of the potential at the origin by an amount given by eq. (6). The choice $c = 1$ for the phenomenological parameter in this equation leads to agreement of the renormalization-group predictions with the lattice results for the properties of the phase transition. For $m_H \gtrsim 40$ GeV the confining regime sets in above the energy scales at which the Coleman-Weinberg mechanism becomes effective. A two-minimum structure is generated, but both minima exist for non-zero values of the Higgs field. The phase transition becomes progressively more weakly first order as the scalar mass is increased. Finally, for a critical scalar mass in the range 80–100 GeV, the two-minimum structure of the potential is no longer expected to appear. The only minimum of the potential exists within the confining region near the symmetric phase. An analytical crossover is expected to replace the first-order phase transition for larger scalar masses.

Acknowledgements: We would like to thank Z. Fodor, M. Shaposhnikov and C. Wetterich for helpful discussions.

References

- [1] D.A. Kirzhnits and A.D. Linde, Phys. Lett. B **42**, 471 (1972); JETP **40**, 628 (1974); Ann. Phys. **101**, 195 (1976); L. Dolan and R. Jackiw, Phys. Rev. D **9**, 3320 (1974); S. Weinberg, Phys. Rev. D **9**, 3357 (1974).
- [2] V.A. Kuzmin, V.A. Rubakov, and M.E. Shaposhnikov, Phys. Lett. B **155**, 36 (1985); M.E. Shaposhnikov, Nucl. Phys. B **287**, 757 (1987); *ibid.* **299**, 797 (1988).
- [3] V.A. Rubakov and M.E. Shaposhnikov, preprint CERN-TH/96-13, hep-ph/9603208; K. Jansen, preprint DESY-95-169, hep-lat/9509018.
- [4] J.E. Bagnasco and M. Dine, Phys. Lett. B **303**, 308 (1993); P. Arnold and O. Espinosa, Phys. Rev. D **47**, 3546 (1993); Z. Fodor and A. Hebecker, Nucl. Phys. B **432**, 127 (1994); K. Farakos, K. Kajantie, K. Rummukainen and M. Shaposhnikov, Nucl. Phys. B **425**, 67 (1994); M. Laine, Phys. Lett. B **335**, 173 (1994); Phys. Rev. D **51**, 4525 (1995); J. Kripfganz, A. Laser and M.G. Schmidt, Phys. Lett. B **351**, 266 (1995).
- [5] A.D. Linde, Phys. Lett. B **96**, 293 (1980); D. Gross, R. Pisarski and L. Yaffe, Rev. Mod. Phys. **53**, 43 (1981).
- [6] W. Buchmüller, Z. Fodor, T. Helbig and D. Walliser, Ann. Phys. **234**, 260 (1994).
- [7] W. Buchmüller and O. Philipsen, Phys. Lett. B **354**, 403 (1995); Nucl. Phys. B **443**, 47 (1995).
- [8] P. Arnold and G. Yaffe, Phys. Rev. D **49**, 3003 (1994).
- [9] Z. Fodor, J. Hein, K. Jansen, A. Jaster, I. Montvay and F. Csikor, Phys. Lett. B **334**, 405 (1994); Z. Fodor, J. Hein, K. Jansen, A. Jaster and I. Montvay, Nucl. Phys. B **439**, 147 (1995).
- [10] F. Csikor, Z. Fodor, J. Hein and J. Heitger, Phys. Lett. B **357**, 156 (1995).
- [11] F. Csikor, Z. Fodor, J. Hein, A. Jaster and I. Montvay, Nucl. Phys. B **474**, 421 (1996).
- [12] K. Kajantie, K. Rummukainen and M. Shaposhnikov, Nucl. Phys. B **407**, 356 (1993); K. Farakos, K. Kajantie, K. Rummukainen and M. Shaposhnikov, Phys. Lett. B **336**, 494 (1994); Nucl. Phys. B **442**, 317 (1995).
- [13] K. Kajantie, M. Laine, K. Rummukainen and M. Shaposhnikov, Nucl. Phys. B **466**, 189 (1996).
- [14] M. Laine, Phys. Lett. B **385**, 249 (1996).

- [15] B. Bunk, E.-M. Ilgenfritz, J. Kripfganz and A. Schiller, Nucl. Phys. B **403**, 453 (1993); M. Gürtler, E.-M. Ilgenfritz, J. Kripfganz, H. Perlt and A. Schiller, preprint UL-NTZ-23/96, hep-lat/9605042.
- [16] N. Tetradis, preprint CERN-TH/96-190, hep-ph/9608272.
- [17] K.G. Wilson and I.G. Kogut, Phys. Rep. **12**, 75 (1974).
- [18] C. Wetterich, Nucl. Phys. B **352**, 529 (1991); Z. Phys. C **57**, 451 (1993).
- [19] C. Wetterich, Phys. Lett. B **301**, 90 (1993).
- [20] M. Reuter and C. Wetterich, Nucl. Phys. B **417**, 181 (1994).
- [21] N. Tetradis and C. Wetterich, Nucl. Phys. B **398**, 659 (1993).
- [22] M. Reuter, N. Tetradis and C. Wetterich, Nucl. Phys. B **401**, 567 (1993); N. Tetradis and C. Wetterich, Nucl. Phys. B **422**, 541 (1994); Int. J. Mod. Phys. A **9**, 4029 (1994); J. Berges, N. Tetradis and C. Wetterich, Phys. Rev. Lett. **77**, 873 (1996); N. Tetradis and D. Litim, Nucl. Phys. B **464**, 492 (1996).
- [23] S. Bornholdt, N. Tetradis and C. Wetterich, Phys. Lett. B **348**, 89 (1995); Phys. Rev. D **53**, 4552 (1996); preprint CERN-TH/96-67, cond-mat/9603129.
- [24] M. Reuter and C. Wetterich, Nucl. Phys. B **391**, 147 (1993); *ibid.* **427**, 291 (1994).
- [25] D. Litim, C. Wetterich and N. Tetradis, preprint HD-THEP-94-23, hep-ph/9407267; B. Bergerhoff, D. Litim, S. Lola and C. Wetterich, Int. J. Mod. Phys. A **11**, 4273 (1996); B. Bergerhoff, F. Freire, D. Litim, S. Lola and C. Wetterich, Phys. Rev. B **53**, 5734 (1996).
- [26] M. Reuter and C. Wetterich, Nucl. Phys. B **408**, 91 (1993).
- [27] B. Bergerhoff and C. Wetterich, Nucl. Phys. B **440**, 171 (1995); preprint HD-THEP-95-37, hep-ph/9508352.
- [28] J. Berges and C. Wetterich, preprint HD-THEP-96-37, hep-th/9609019; J. Berges, N. Tetradis and C. Wetterich, preprint CERN-TH/96-289, hep-ph/9610354.
- [29] U. Ellwanger, M. Hirsch and A. Weber, Z. Phys. C **69**, 687 (1996); preprint LPTHE-ORSAY-96-50, hep-ph/9606468; D.U. Jungnickel and C. Wetterich, Phys. Rev. D **53**, 5142 (1996); preprint HD-THEP-96-19, hep-ph/9606483.
- [30] J. Adams, J. Berges, S. Bornholdt, F. Freire, N. Tetradis and C. Wetterich, Mod. Phys. Lett. A **10**, 2367 (1995).
- [31] S. Coleman and E. Weinberg, Phys. Rev. D **7**, 1888 (1973).

- [32] U. Ellwanger, Z. Phys. C **58**, 619 (1993); U. Ellwanger and C. Wetterich, Nucl. Phys. B **423**, 137 (1994).
- [33] M. Reuter and C. Wetterich, preprint HD-THEP-94-39, hep-th/9411227.
- [34] T. Banks and E. Rabinovici, Nucl. Phys. B **160**, 349 (1979); E. Fradkin and S.H. Shenker, Phys. Rev. D **19**, 3682 (1979).
- [35] K. Kajantie, M. Laine, K. Rummukainen and M. Shaposhnikov, Phys. Rev. Lett. **77**, 2887 (1996).

Figures

Fig. 1 The effective average potential $U_k(\rho, T_{cr})$, for the $SU(2)$ Higgs model with $e_R^2 = 0.1073$, $m_W = 80.6$ GeV, $m_H = 35$ GeV, as the coarse-graining scale k is lowered.

Fig. 2 The effective average potential $U_k(\rho, T_{cr})$, for the $SU(2)$ Higgs model with $e_R^2 = 0.1073$, $m_W = 80.6$ GeV, $m_H = 70$ GeV, as the coarse-graining scale k is lowered.

Fig. 3 The location of the two minima of the potential at the critical temperature, as a function of the Higgs boson mass, for $m_W = 80.6$ GeV. The boxes correspond to $e_R^2 \simeq 0.107$ and the stars to $e_R^2 \simeq 0.145$.

Tables

e_R^2	0.1463	0.1446	0.1073	0.1073
m_H/GeV	34	49	29.1	54.4
T_{cr}/GeV	77.5	103	78.7	130
T_{cr}/m_H	2.28	2.10	2.71	2.39
$\phi_0(T_{cr})/\text{GeV}$	110	114	118	119
$\phi_{np}(T_{cr})/\text{GeV}$	—	31.2	—	31.7
$\Delta\phi(T_{cr})/T_{cr}$	1.42	0.804	1.50	0.672
k_{conf}/GeV	13.0	17.3	10.1	16.6
$m_W(\rho_{0R}, T_{cr})/\text{GeV}$	44.9	47.1	41.3	43.9
$m_H(\rho_{0R}, T_{cr})/\text{GeV}$	13.8	21.8	10.1	21.6
$\sigma/(\text{GeV})^3$	3.04×10^4	4.75×10^4	2.63×10^4	5.36×10^4
σ/T_{cr}^3	6.53×10^{-2}	4.35×10^{-2}	5.40×10^{-2}	2.44×10^{-2}
$\Delta Q/(\text{GeV})^4$	6.84×10^6	1.63×10^7	6.07×10^6	1.86×10^7
$\Delta Q/T_{cr}^4$	1.90×10^{-1}	1.45×10^{-1}	1.58×10^{-1}	6.51×10^{-2}

Table 1: Characteristics of the first-order phase transition for the $SU(2)$ Higgs model with $m_W = 80.6$ GeV.

	RG1	RG2	L1	L2	PT1	PT2
T_{cr}/GeV	77.5	79.6	73.0(14)	75.7(5)	78.2	78.0
σ/T_{cr}^3	0.0653	0.0274	0.053(5) ($L_t = 2$)	0.050(12)	0.027	0.056
$\Delta Q/T_{cr}^4$	0.190	0.120	0.28(12) ($L_t = 4$)	0.19(1)	0.13	0.19

Table 2: Comparison of results from renormalization-group, lattice and perturbative studies for $e_R^2 = 0.1463$, $m_W = 80.6$ GeV, $m_H = 34$ GeV.

RG1: Integration of the evolution equation for the potential, with the contribution of the strongly coupled regime around the origin approximated by eq. (6) with $c = 1$.

RG2: The same as for RG1, but with $c = 0.5$.

L1: Lattice study of refs. [10, 11]. The continuum limit $L_t = \infty$ has been studied only for T_{cr} .

L2: Extrapolated results [14] of the lattice study of ref. [13].

PT1: Perturbation theory to order e^3 [11].

PT2: Perturbation theory to order e^4 [11].

	RG	L1	RG	L2	RG	L3	RG	L3
e_R^2	0.1463		0.1446		0.1073		0.1073	
m_H/GeV	34		49		29.1		54.4	
T_{cr}/GeV	77.5	73.0(14)	103	[92.9(13)]	78.7	76.8(5)	130	132.6(5)
σ/T_{cr}^3	0.0653	[0.053(5)]	0.0435	[0.008(2)]	0.0540	[0.071(3)]	0.0244	0.0017(4)
$\Delta Q/T_{cr}^4$	0.190	[0.28(12)]	0.145	[0.122(9)]	0.158	0.200(7)	0.0651	0.0294(7)

Table 3: Comparison of results from renormalization-group and lattice studies for $m_W = 80.6$ GeV.

RG: Integration of the evolution equation for the potential.

L1: Lattice study of refs. [10, 11].

L2: Lattice study of ref. [9]. The results correspond to values of e_R^2 slightly different from the one quoted in the first row.

L3: Lattice study of ref. [13].

For the results in brackets, the continuum limit has not been studied.

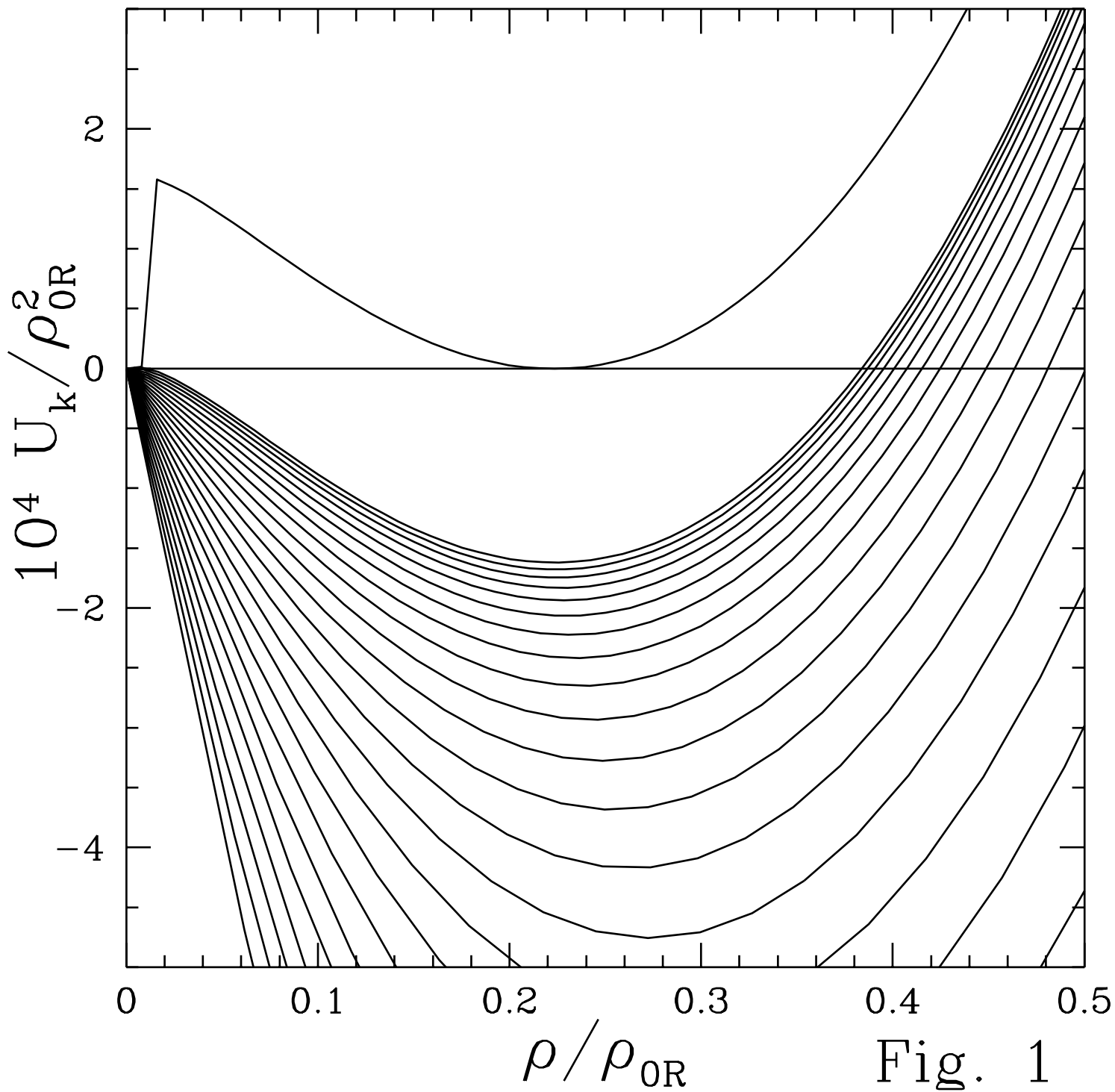


Fig. 1

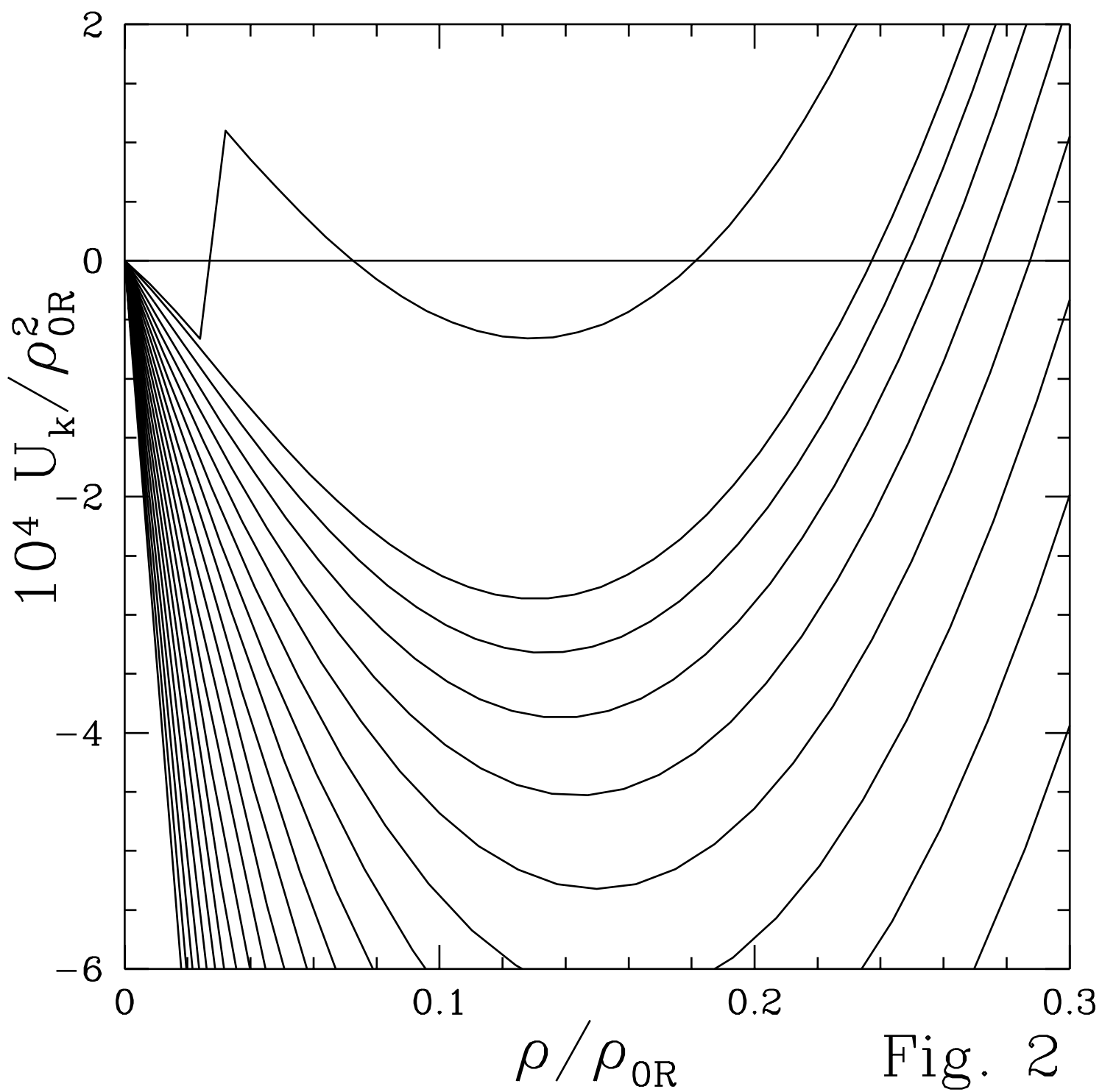


Fig. 2

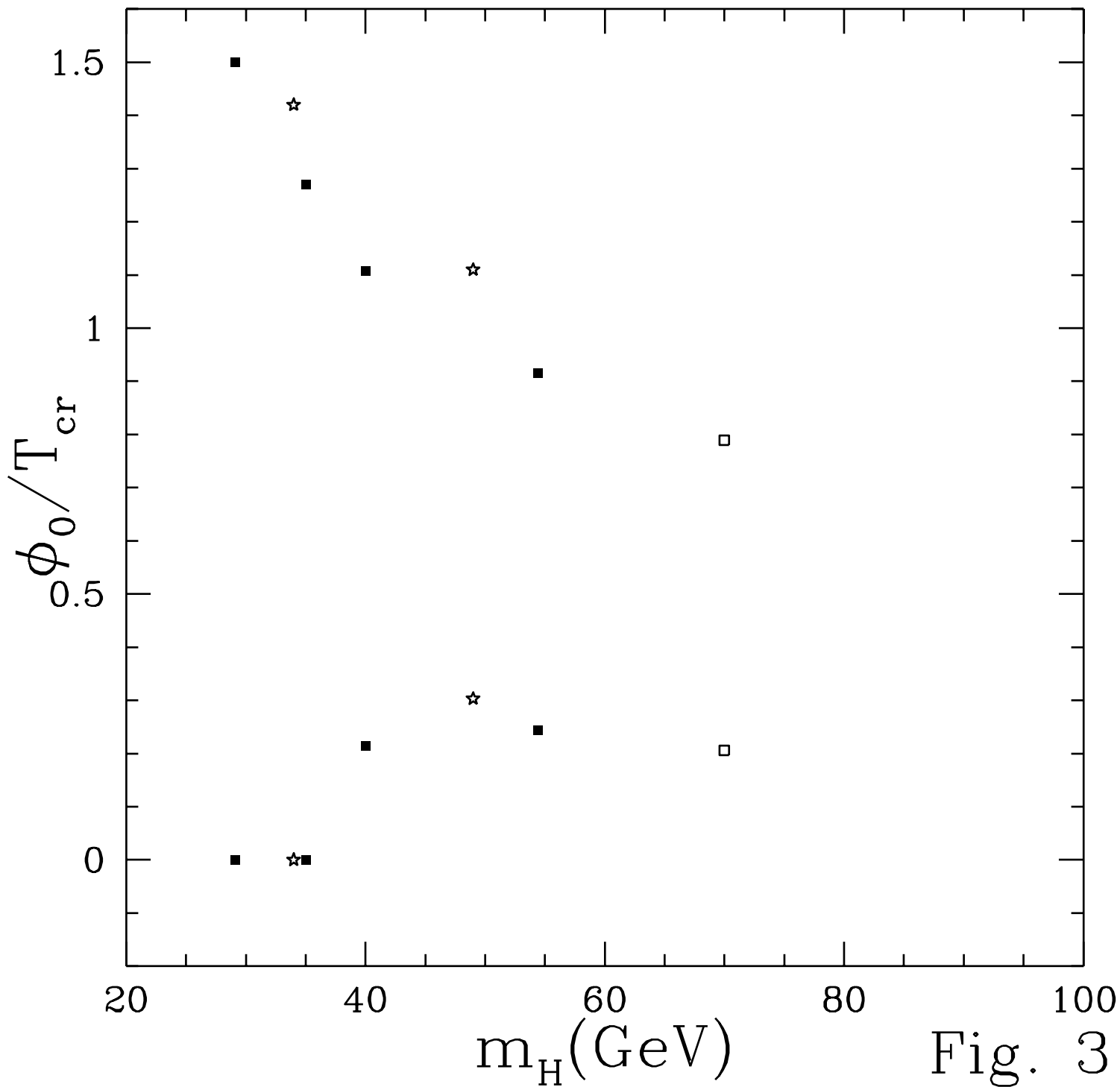


Fig. 3